 doi:10.20944/preprints202206.0379.v1

Article

Porous TiO_2/Carbon Dots Nanoflowers with Enhanced Surface Areas for Improving Photocatalytic Activity

Fengyan Song [2], Hao Sun [1,3,4], Hailong Ma[1,3,4] and Hui Gao [1,3,4]*

[1] Ningbo Institute of Technology, Beihang University, Ningbo 315100, P. R. China
[2] Center of Excellence for Environmental Safety and Biological Effects, Beijing Key Laboratory for Green Catalysis and Separation, Department of Chemistry and Biology, School of Life Science and Chemistry, Faculty of Environment and Life, Beijing University of Technology, Beijing, 100124, China.
[3] School of Aeronautic Science and Engineering, Beihang University, Beijing, 100191, China.
[4] Hangzhou Innovation Institute (Yuhang)– Beihang University, Hangzhou, Zhejiang, 310052, China
* Correspondence: h.gao@buaa.edu.cn

Abstract: Electron-hole recombination and narrow range utilization of sunlight limit the photocatalytic efficiency of TiO_2. We synthesized a carbon dots (CDs) modified TiO_2 nanoparticles (NPs) with flower-like mesoporous structure, *i.e.*, porous TiO_2/CDs nanoflowers. Among such hybrid particles, CDs worked as photosensitizers for the mesoporous TiO_2 and enabled the resultant TiO_2/CDs nanoflowers with a wide-range light absorption. Rhodamine B (Rh-B) was employed as a model organic pollutant to investigate the photocatalytic activity of the TiO_2/CDs nanoflowers. The results demonstrated that the decoration of CDs on both TiO_2 nanoflowers and P25 NPs enabled a significant improvement of the photocatalytic degradation efficiency compared with the pristine TiO_2. TiO_2/CDs nanoflowers with porous structure and larger surface areas than P25 showed a higher efficiency owing to prevent local aggregation of carbon materials. All the results revealed that the introduced CDs and the unique mesoporous structure, large surface areas and loads of pore channels of the prepared TiO_2 NPs played important roles in the enhancement of the photocatalytic efficiency of the TiO_2/CDs hybrid nanoflowers. Such TiO_2/CDs composite NPs also opens a door for photodegradation, photocatalytic water splitting and enhanced solar sunlight as light source.

Keywords: porous TiO_2; hybrid TiO_2/CDs; photocatalysts; photodegradation; large surface areas

1. Introduction

The pollutants, such as inorganic nitrogen oxides and organic dyes from gas or liquid phases, may cause severe environmental and health problems, hence complete degradation and elimination of them is of great importance.[1-3] Removal of pollutants via photocatalytic oxidation process using semiconductor materials and harnessing solar energy has been gaining increasing interest in the last decade, because it is a promising green technology.[4-5] Among them, titanium oxide (TiO_2)-based materials are believed to be the most reliable materials for photocatalytic reactions due to its low toxicity, high chemical stability, availability, abundance and low cost.[6-9] However, the application of pure TiO_2 is limited by its relative low solar photo-conversion efficiencies, because its wide band gap (3.2 eV for anatase and 3.0 eV for rutile) requires photocatalytic activation only by ultraviolet irradiation (< 4% of the total solar spectrum),[10] and the high electron-hole recombination rate in TiO_2 particles results in low quantum efficiency of photocatalytic reactions.[11] Therefore, great efforts have been directed towards modifying TiO_2 to extend its photocatalytic activity into the visible region and supress the recombination of photo-generated electro-hole pairs, and thereby enhance solar energy conversion and improve the photocatalytic efficiency. To achieve this target, various strategies have been adopted including doping with transition metals ions (*e.g.* V, Cr, Fe),[12] coupling with narrow band gap semiconductors,[13-14] depositing noble metals,[15-16] and incorporation of non-metal elements.[3, 6, 17-19] Doping TiO_2 with metal ions narrowed the bandgap due to the formation of

Preprints (www.preprints.org) | NOT PEER-REVIEWED | Posted: 28 June 2022 doi:10.20944/preprints202206.0379.v1

intermediate energy levels in the band gap.[6] However, the metal doped materials lack the necessary thermal stability, exhibit atom diffusion and a remarkably increased electron/hole recombination of defect sites, which results in a low photocatalytic efficiency.[12] Non-metal doping TiO_2 has since been proved to be far more successful, and numerous reports on TiO_2 doped with B, F, N, S, I and C have demonstrated a significant improvement of the visible-light photocatalytic efficiency.[1, 11, 20-21]

Among these, the decoration of TiO_2 with carbonaceous nanomaterials like carbon nanotube,[22] C60,[23-24] graphene,[25-26] *etc.* is being increasingly investigated. The resultant TiO_2/carbon composites were demonstrated in the literature with an improved optical absorbance and better photocatalytic activities in the visible light range when compared with pristine TiO_2.[6, 27] Carbon dots (CDs), 0-D nanodots, have recently emerged as a new member of the nano-carbon family, and have drawn great attention due to their unique properties.[28-29] Like traditional semiconductor quantum dots, CDs show excellent photoluminescence, great resistance to photo-bleaching and good chemical stability. In addition, they possess the advantages of well water dispersibility, non-toxicity, electron-accepting and transport properties, and facile production of low cost. [30-31] To date CDs have been applied to couple with TiO_2 to extend their light absorption to visible range for a better photocatalytic performance. Researcher believed that CDs can improve optical absorption, trap charge carrier, and hinder the recombination of the photo-generated electron-hole pairs.[32-37] In addition CDs with up-conversion property may even broaden their absorption to NIR light range and enable them with NIR photocatalytic activity.[33] However, up to now, most of the reported TiO_2/CDs photocatalysts were mainly focused on employing TiO_2 particles with nanotube, nano-belts, or spherical morphology.[32-35] These TiO_2 nanocomposites are normally possess low surface areas which tends to cause uneven distribution and local aggregation of carbon materials, making them the recombination center of photo-generated carriers, reducing the utilization of light.[11]

To solve this problem, we introduce wide visible to NIR absorption range CDs into the mesoporous TiO_2 matrix with precise pore size of around 5 nm to simultaneously utilize the advantages of CDs and mesoporous structured materials with high surface areas. The porous structure and high surface areas may increase the effective contact areas between the pollutants and the active surfaces of photocatalytic particles, reducing local CDs aggregate, which can significantly improve catalytic efficiency.[22] Herein, TiO_2 with mesoporous structure and higher surface areas than the commercial P25 TiO_2 was synthesized by using hydrothermal method and calcination method. CDs were fabricated by simple hydrothermal carbonation of biomass, and then introduced them into the mesoporous TiO_2 particles by self-assembly process, thereby forming TiO_2/CDs hybrid particles. The photocatalytic behaviour of as-synthesized TiO_2 and TiO_2/CDs samples towards the degradation of rhodamine B (Rh-B) were studied and exhibit higher catalytic efficiency compared to the commercial P25 TiO_2.

2. Materials and Methods

2.1. Preparation of TiO_2 mesoporous particles.

2 mL of titanium butoxide was dispersed in a solution of 20 mL NH_3H_2O (37%) dissolved with 0.28 g KCl. The suspension was stirred for 30 minutes, transferred to Teflon-sealed autoclave reactor and maintained at 180 ^oC for 4 h. The precipitates were then washed with ethanol and DI-water for a few times to remove free ions, and freeze-dried. Finally, the resulting dry powder was calcined by a conventional method, in which the calcinations was conducted at temperature at 550 ^oC for 4 h in air with a heating ramp of 10 ^oC/min.

2.2. Preparation of carbon dots.

0.7 g D-(+)-glucose was dissolved in 20 mL ethanol and placed in a Teflon-lined, stainless steel autoclave, which underwent treatment at 200 ^oC for 6 h. The dark brown and yellow solution obtained was centrifuged at 10000 rpm for 20 min to remove the

 doi:10.20944/preprints202206.0379.v1

solution containing fluorescent CDs from the solid black precipitate. The solution of CDs was then filtered using standard syringe filters.

2.3. Preparation of TiO_2/CDs photocatalysts.

The as-prepared mesoporous TiO_2 particles were coated with CDs by soaking them in the CD solution in ethanol for 24 h before removing and rinsing with clean ethanol to remove any poorly adhered CDs.

2.4. Characterization of the photocatalysts.

Several techniques were employed for the characterization of the samples. In order to determine the crystal phase composition of the as-prepared TiO_2 particles, X-ray diffraction measurements were carried out at room temperature using a Bruker D5000 with Cu Kα radiation in the region 2θ= 15-70°. The morphology and surface characteristics of the TiO_2 particles were investigated by using a Scanning Electron Microscopy (SEM, FEI Inspect-F). Samples were observed using an accelerating voltage of 20 kV, a spot size of 3.5, and a working distance of approximately 10 mm. The microcrystalline morphology and structure of the samples was analysed by Transmission Electron Microscopy (TEM) and High-Resolution (HR) TEM, using a JEOL JEM-2010 electron microscope operating at 200 kV. BET surface area determination was obtained by measuring N_2 adsorption–desorption isotherm using an Autosorb-IQ2-MP-C system (Quantachrome Instruments, USA). During the BET analysis, the samples were degassed at 150 °C for 24 h prior to nitrogen adsorption measurements. The specific surface area was calculated by the multipoint Brunauer–Emmett–Teller (BET) method, and the pore-size distribution was calculated based on Quenched Solid Density Function Theory (QSDFT) using the adsorption branch. Absorption spectra of the products (CDs, TiO_2, and TiO_2/CDs hybrid particles) were measured using PerkinElmer Lambda LS 35 UV/Vis spectrometer. The fluorescence spectra of CDs and TiO_2/CDs were measured using the fluorescence spectrometer PerkinElmer LS 55, with a slit width of 10 nm both for excitation and emission. Fourier transform infrared (FTIR) spectra were recorded on FTIR spectrometer 100, Perkin-Elmer, collecting data canning from 4000 to 400 cm^{-1} at a spectral resolution of 4 cm^{-1}.

2.5. Photocatalytic degradation experiments.

The photocatalytic activity of the synthesized pure TiO_2 and TiO_2/CDs was tested under a Xenon lamp (λ > 340 nm, ~110 mW cm^{-2}). Rh-B solution with concentration at 20 μg/mL was prepared in DI-water. Typically, 10 mg powder samples were suspended in 30 mL Rh-B solution. Prior to the light irradiation, the suspension was kept in the dark for 30 min under magnetic stirring to reach the adsorption–desorption equilibrium between Rh-B molecules and the photocatalysts. Then the above suspension kept in a quartz cuvette was exposed to the irradiation light (λ > 340 nm). An ice bath was applied to ensure that the temperature change of the suspensions was less than 5 °C. With magnetic stirring, 3 mL of the dispersion was taken out at regular intervals and centrifuged at 10000 rpm for 5 min, and then the supernatant solution was collected and analysed using a UV-Vis absorbance spectroscopy. For comparison, the photocatalytic reactions were carried out with the catalyst of P25 and P25/CDs under the same procedure. The percentage of degradation was calculated as C_t/C_0, where C_t is the concentration of the remaining dye solution at each irradiated time interval, while C_0 means the concentration of Rh-B solution after keeping it in the dark for 30 min in the presence of any photocatalyst.

3. Results and Discussion

As depictured in Scheme 1, the synthesis of porous TiO_2/CDs photocatalyst was realized with a few steps. The TiO_2 with porous structure was fabricated through a combined hydrothermal reaction (180 °C) and calcination method (550 °C), using titanium butoxide, KCl and NH_4OH as starting materials. The TiO_2 allows a controlled interface and nanocrystal growth under such high thermal treatment. CDs were produced by

Preprints (www.preprints.org) | NOT PEER-REVIEWED | Posted: 28 June 2022 doi:10.20944/preprints202206.0379.v1

hydrothermal carbonisation of D-(+)-glucose at 200 °C and were simply introduced into porous TiO_2 by self-assembly method. The formed TiO_2/CDs was then used for degradation study of organic dyes.

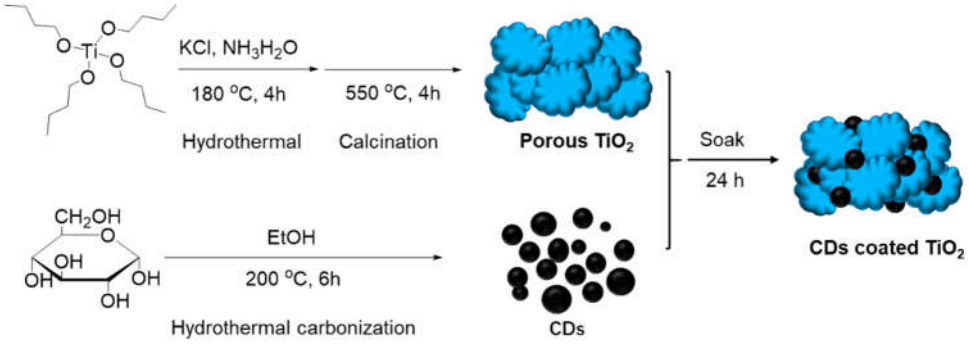

Scheme 1. Schematic diagram of hybrid TiO_2/CDs preparation procedure.

XRD measurement of the as-prepared TiO_2 particles was carried out to investigate their crystalline structure as shown in Figure 1a. XRD pattern exhibited strong diffraction peaks at 25.4°, 37.8°, 48°, 53.9°, 55.1° and 62.7°, which correspond to (101), (004), (200), (105), (211), and (204) faces of anatase TiO_2.[38] Notably, there were no apparent peaks at the position of 27.58°, 41.38, 44.18, which are the characteristic peaks for rutile TiO_2. It shall be mentioned that anatase and rutile are two type of TiO_2 polymorphs which are typically being used for photocatalytic application. Anatase structure is preferred due to its significantly higher photocatalytic activity than the rutile phase for several reasons: (1) anatase has a larger band-gap than rutile, which provides anatase with a higher redox potential; (2) anatase has a higher area density of surface hydroxyls, which slows the recombination rate of photogenerated electron-hole pairs.[22, 28] Even though the real causes of the better photocatalytic properties of anatase are not yet fully understood, it is speculated that charge-carrier mobility in anatase is 89 times faster than that in rutile, which is around 80 $cm^2\ V^{-1}\ s^{-1}$.[22, 39-40]. Hence, we expected that the as-synthesised TiO_2 particles that were mainly composed of anatase phase TiO_2 may possess a superior photocatalytic activity. The scanning electron microscopy (SEM) image showed porous and aggregated particles which were self-assembled by petal-shaped TiO_2 nanoparticles (Figure S1a), while the transmission electron microscopy (TEM) image in Figure 1b displayed a network of porous interconnected channels due to these constituent agglomerated petal-shaped TiO_2 nanoparticles, demonstrating a sponge-like and mesoporous architecture. High resolution (HR)-TEM image of the TiO_2 materials showed clear lattice fringes of the TiO_2 particles, indicating an interplanar spacing of 0.35 nm (Figure 1c), which matched well with the (101) plane of anatase TiO_2. In addition, our HRTEM image indicated the crystallite of TiO_2 are in indeed nano-sized and the aggregated particles were with through pore structures formed by these nanocrystals, as can be verified from the contrasts in the HRTEM image (Figure 1c). The crystallographic structure of the TiO_2 material was further characterized by selected area electron diffraction (SAED), as displayed in Figure 1d**.** With a bright 101 ring, the diffraction rings can be indexed perfectly to the anatase phase of TiO_2.[41] Both the HRTEM and SAED analyses demonstrated a perfectly crystallized TiO_2 materials, which was correspondent well with the XRD results.

Preprints (www.preprints.org) | NOT PEER-REVIEWED | Posted: 28 June 2022 doi:10.20944/preprints202206.0379.v1

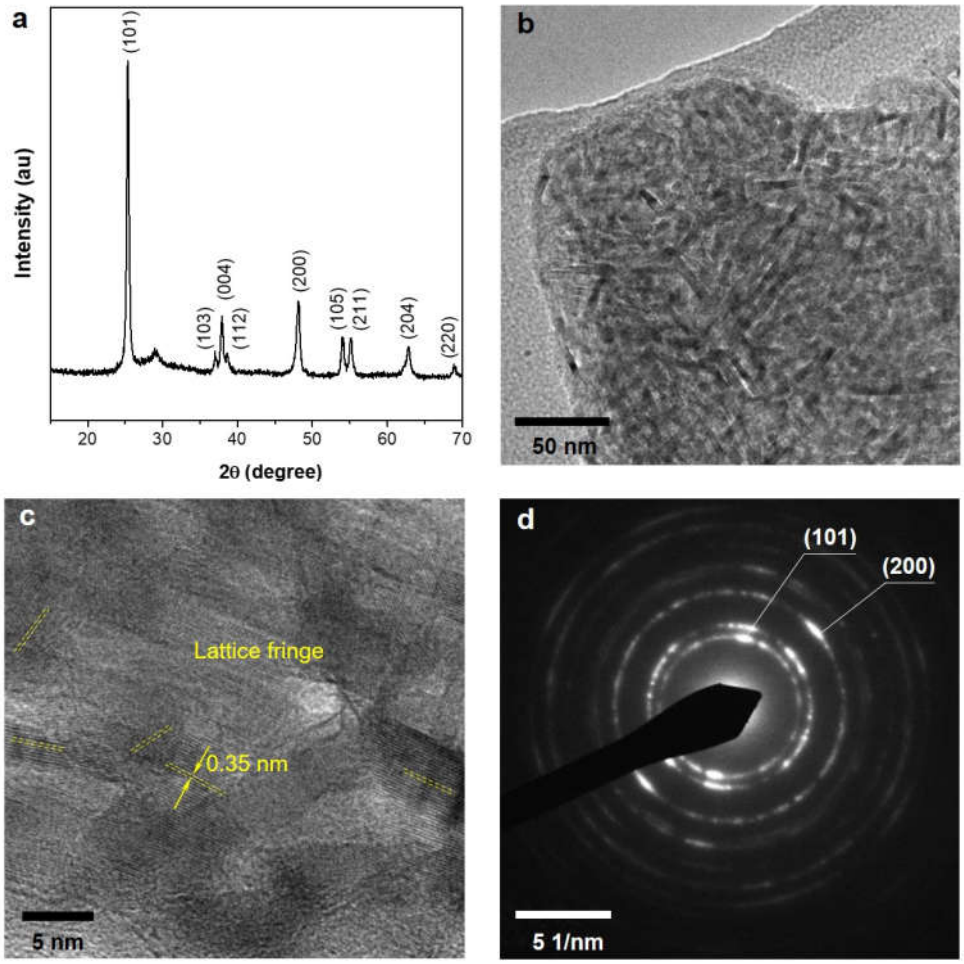

Figure 1. (a) XRD spectra of the obtained porous TiO_2 (b) transmission electron microscopy (TEM) image, (c) High Resolution Transmission Electron Microscope (HRTEM) image and (d) selected area electron diffraction (SAED) pattern of the porous TiO_2.

When CDs were introduced into porous TiO_2 by self-assembly method, porous TiO_2/CDs nanoflowers structures were formed (Figure S1b). To confirm that the porous TiO_2 are incorporated with CDs, Energy Dispersive X-ray (EDX) spectrometry were conducted. Peaks of C, O and Ti elements are shown in the EDX spectra of hybrid TiO_2/CDs nanoflowers (Figure. S2), in which C is from the assembled CDs, demonstrating that CDs is successfully incorporated into the porous TiO_2. Therefore, CDs coated porous TiO_2 are successfully fabricated. (TEM) image also confirmed that a network mesoporous architecture of porous interconnected channels with carbon dots incorporated (Figure 2a). HRTEM image of the TiO_2/CDs showed a clear lattice spacing of 0.35 nm which corresponded to the (101) plane of anatase TiO_2 (Figure 2b) and the interface of amorphous carbon dots and continuous lattice fringes TiO_2 (Figure 2b).

Preprints (www.preprints.org) | NOT PEER-REVIEWED | Posted: 28 June 2022 doi:10.20944/preprints202206.0379.v1

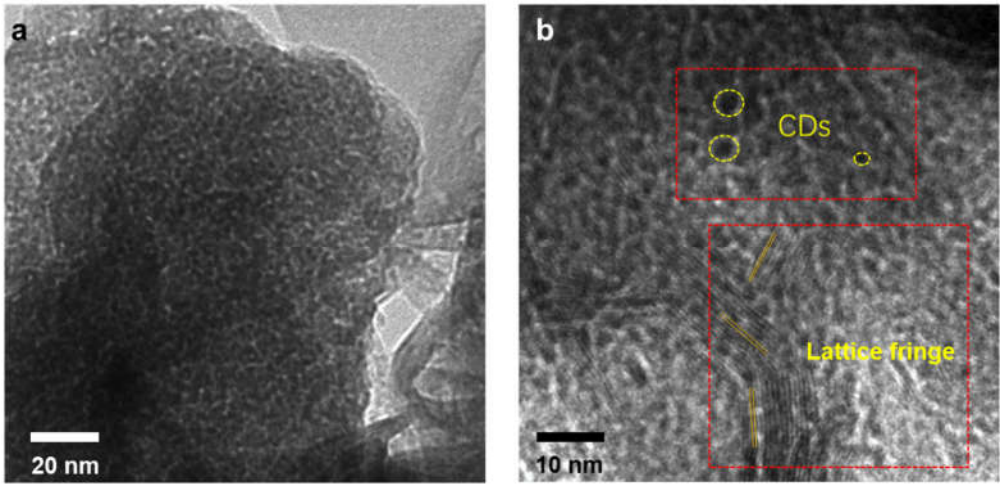

Figure 2. (a) TEM image and (b) HRTEM image of porous carbon dots/TiO_2.

The surface area and the pore characteristics of the TiO_2 product were investigated by measuring the nitrogen isotherms (adsorption-desorption loop), as shown in Figure 3a. The hysteresis loop of the prepared TiO_2 demonstrated a typical type IV isotherm, revealing the characteristic of mesoporous materials. The specific surface area of porous TiO_2 was calculated to be 235.86 m^2/g, which is greatly larger than the commercial TiO_2 (P25) (50 m^2/g, data provided by manufacturer). The pore size distribution of the sample was determined by the Barret-Joyner-Halenda (BJH) equation[42], which suggested a well-defined porous structure (Figure 3b). Pore size distribution shows that the majority of the pores are around 5 nm in diameter, consistent with our HRTEM results. The BET results also showed that the mesoporous channels remain open. Such open mesoporous architecture with connected pore system and large surface area plays an important role in catalyst design for the ability to improve molecular transport of reactants and products.[27] After integrated with CDs, the surface area decreased to 124.923 m^2/g. The average pore size reduced to 1.07 nm, revealing the CDs were incorporated into the large pores of TiO_2.

The UV-vis absorption spectra of the pure CDs, pure porous TiO_2 and TiO_2/CDs were shown in Figure 3c-d. Pure CDs exhibited two strong absorption peaks in the UV region tailing into the visible range until λ = 550 nm. The curves of porous TiO_2 and TiO_2/CDs showed strong light absorption at the UV and visible wavelength of 200-800 nm. Notably, compared with pure porous TiO_2, the TiO_2/CDs showed a wider peak and higher absorption intensity, indicating a significant enhancement of light absorption. The peak position of porous TiO_2 located at ~290 nm, while that of TiO_2/CDs shifted to ~365 nm. Similarly, P25 TiO_2 with CDs incorporation demonstrated a broader peak, higher absorption intensity and a longer wavelength of the peak position then pure P25 TiO_2, as can be seen from Figure S3. For both our synthesized TiO_2 and the commercial P25 TiO_2, their light absorbance was extended and enhanced with the import of CDs. The reason for the enhancement of the UV and visible light absorption could be attributed two parts: (1) the TiO_2/CDs performed like ''dyade'' structure, where the TiO_2 and CDs may form a joint electronic system, which gave rise in synergistic properties;[6] (2) the CDs themselves which could absorb UV light and part of visible light.[10] The above results indicated that we demonstrated the design of photocatalysts to enable to harness the use of the full spectrum of sunlight. The porous TiO_2 with high surface area possessed better absorbance of the UV light and even the visible light than the commercial P25. Moreover, the sensitization of TiO_2 with CDs could significantly enhance their UV-vis light absorption and reduce the extinction in the IR region. The as-prepared pure CDs exhibited an excitation-dependent down-conversion photoluminescent (PL) behaviour (Figure S4). It is interesting that no position shift of PL emission peaks of TiO_2/CDs upon excitation from 280 nm to 800 nm (Figure 3d). The peak is around 512 nm, which further proved the TiO_2/CDs photocatalyst could absorb wide spectrum of sunlight. Moreover, the maximum emission for TiO_2/CDs was found at 460

Preprints (www.preprints.org) | NOT PEER-REVIEWED | Posted: 28 June 2022 doi:10.20944/preprints202206.0379.v1

nm excitation, which further confirmed that the CDs attached on porous TiO_2 has a prefer absorbance at 460 nm. This also amplify the photocatalytic property of the composite.

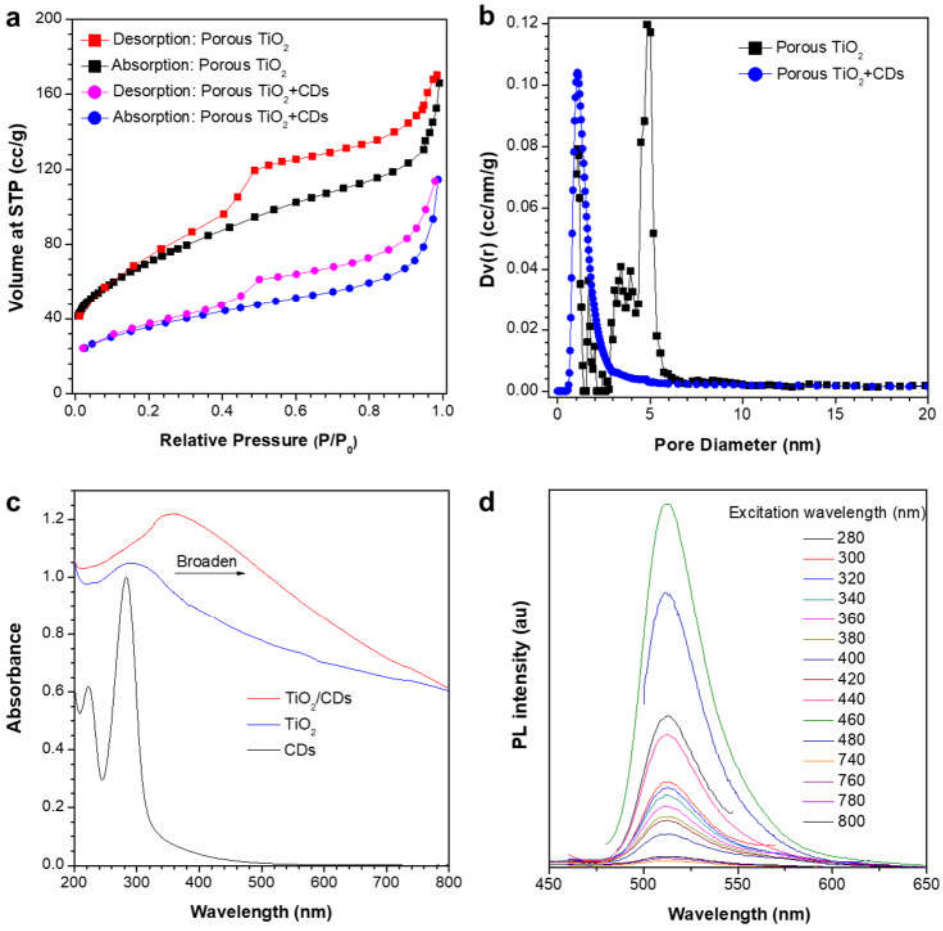

Figure 3. (a) Nitrogen adsorption-desorption isotherm curves of porous TiO_2 and porous TiO_2/CDs particles. (b) Pore size distribution curves of the porous TiO_2 and porous TiO_2/CDs particles. (c) UV-Vis of CDs (from D-glucose with ethanol), porous TiO_2 and porous TiO_2/CDs nanocomposite particles. (d) Photoluminescence spectrums of the porous composite TiO_2/CDs (add up-conversion).

The photocatalytic activities of the prepared porous TiO_2 and porous TiO_2/CDs samples were evaluated by the degradation reaction of organic dye Rh-B. The concentration of Rh-B was calculated as a function of the irradiation time by measuring the absorbance intensity changes at 554 nm with a UV–vis spectrophotometer. To eliminate the influence caused by adhering of Rh-B on the surface of composite NPs, samples were permitted to be fully saturated with Rh-B solution in dark environment under magnetic stirring until the Rh-B concentration of the supernatants remained constant. After full adsorption in the pores, the photocatalytic activities of the samples were evaluated by measuring the time-dependent photodecomposition of Rh-B aqueous solutions upon the irradiation, as shown in Figure 4a,b. The absorption intensity at λ = 553 nm decreased significantly for both sample systems when prolonging the irradiation time. It was found that, TiO_2 incorporated with CDs worked more effective for Rh-B degradation. After 90 mins of irradiation, Figure 4c showed that around 40% of Rh-B was still maintained in the pure TiO_2 system, however, only around 10% of Rh-B was not degraded in the TiO_2/CDs system. The degradation rates of Rh-B dye over TiO_2 without and with CDs incorporation. The corresponding degradation rates of Rh-B dye over different samples were displayed in Figure 4d, indicating a higher degradation rate of TiO_2/CDs than that of TiO_2. In addition, contrast experiments were carried out using commercial P25 as photocatalysts, and the same procedure for the reduction of Rh-B was employed (Figure S5). P25 TiO_2 with CDs

Preprints (www.preprints.org) | NOT PEER-REVIEWED | Posted: 28 June 2022 doi:10.20944/preprints202206.0379.v1

incorporation demonstrated a better degradation efficiency and a higher degradation rate. The results indicated that around 22% of Rh-B in P25/CDs sample while around 50% in P25 samples were left after 90 mins irradiation.

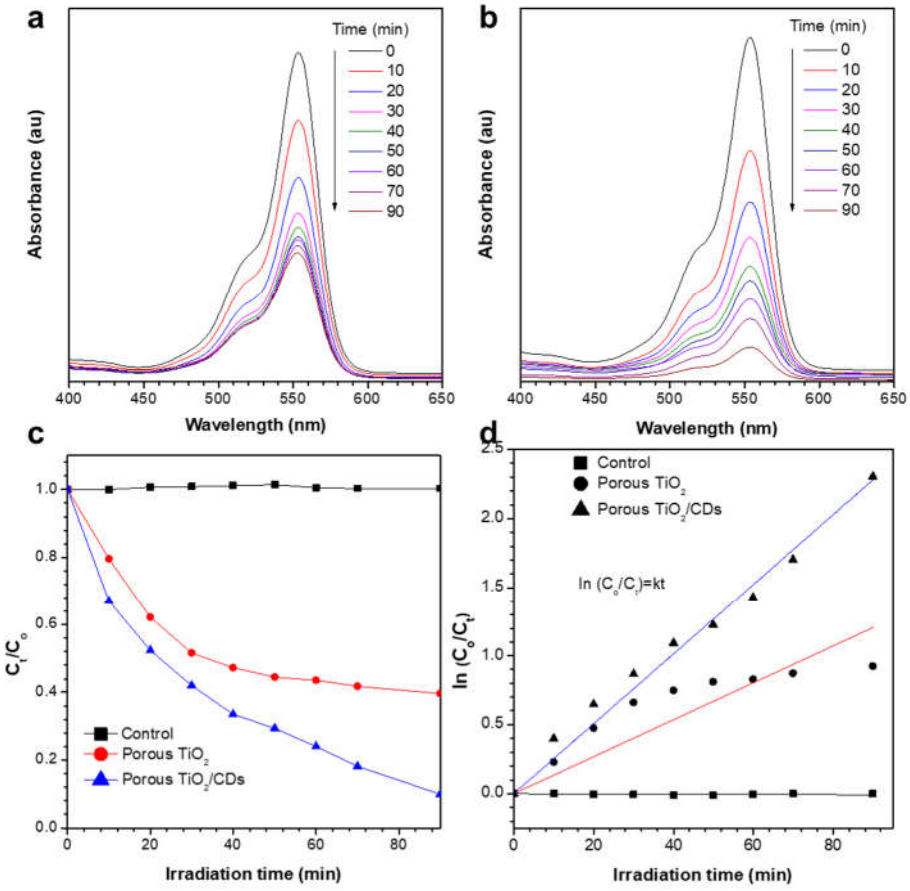

Figure 4. UV-Vis spectra of RhB-degradation with (a) porous TiO_2 and (b) porous TiO_2/CDs under light irradiation for different time. (c) Photocatalytic degradation curves of porous TiO_2 and porous TiO_2/CDs at different time under light irradiation. (d) Pseudo-first-order fitted degradation of RhB by porous TiO_2 and porous TiO_2/CDs.

The above analysis revealed that both the synthesized TiO_2 and commercial P25 TiO_2 samples with CDs showed the higher photocatalytic activity of the corresponding bare TiO_2 materials upon the light irradiation, thus proving that indeed a special behaviour is to be expected, due to the intrinsic properties of CDs and the possible interaction between the CDs and TiO_2. The possible mechanism could be explained as follows. Firstly, CDs incorporation could increase the amount of the total light absorption, which should be from both CDs and Ti species. As demonstrated in Figure 3c, the absorption edge of the TiO_2 exhibits red-shifted after bonding with CDs, indicating that the hybrid TiO_2/CDs particles have an extended light absorption spectrum and can absorb more light during the photocatalytic process. Secondly, CDs could create an intragap localized states of C 2p situated around the valence band edge of TiO_2 (Figure 5),[30] and NIR light irradiated on CDs can be up-converted to visible light (Figure 3d), therefore, the Ti species could also be excited by the visible light and even the NIR light so as to produce electron-hole pairs and generate $\cdot O_2^-$ and ·OH. Thirdly, CDs are able to serve as electron acceptors and donors,[20] wherein the photo-induced electrons can transfer from CDs to TiO_2 surfaces, and then the redundant electrons on TiO_2 can transfer back to the CDs, as illustrated in Figure 5. To be more precise, on the one hand, CDs can serve as electron reservoirs to trap the photo-induced electrons from TiO_2, facilitating the efficient separation of electrons and holes and thereby improving their photocatalytic activity. On the other hand, CDs could

Preprints (www.preprints.org) | NOT PEER-REVIEWED | Posted: 28 June 2022 doi:10.20944/preprints202206.0379.v1

work as photosensitizes to TiO_2, sensitizing TiO_2 through the possible formed Ti–O–C bond between the TiO_2 and CDs, and inject the photo-generated electrons to the conduction band of TiO_2.[43] When the electron is transferred to surface-absorbed O_2, active specie of $\cdot O_2^-$ will form. Consequently, the integration of CDs and TiO_2 could efficiently promote the transfer of photo-generated electrons, reduced the electron-hole recombination rate, and then greatly enhance the generation of active species on the surface.[30] Furthermore, the synthesized TiO_2/CDs demonstrated better photocatalytic activity than P25/CDs sample, demonstrating that the microstructure of particles plays an important role in their efficient photocatalytic activity. Specifically, mesopores in TiO_2 particles influenced the photocatalytic effect to a great extent, which was mainly due to two aspects: (1) large surface area resulting from the mesoporous structure provided plenty of active sites and enabled a better adsorption of the Rh-B molecules; (2) mesoporous channels provided paths for dye molecules to diffuse easily and reach to the active sites.[44] The larger surface area of porous TiO_2 was prove by the BET data (Figure 3a,b). All the above proposed causes contributed to the final excellent photocatalytic activity of the porous TiO_2/CDs hybrid materials.

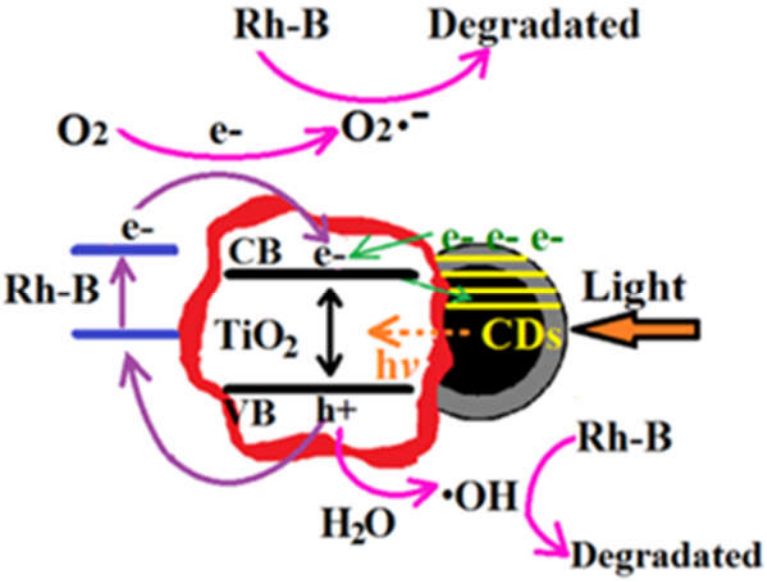

Figure 5. Schematic description of the proposed photocatalysis mechanism.

4. Conclusions

We hope that the present strategy for constructing CPL-active materials in the condensed matter states will open numerous opportunities for applications in photonic devices. The photo-degradation of Rh-B demonstrated an excellent photocatalytic activity of the TiO_2/CDs hybrid particles, which was much higher than the pristine porous TiO_2. With CDs incorporation, P25 also showed an increased photocatalyatic activity than that without CDs. It's believed that new chemical and optical properties of the TiO_2/CDs nanohybird were introduced by CDs, which synchronously made a great contribution to the enhanced photocatalytic activity. The photocatalytic differences between mesoporous TiO_2/CDs and P25/CDs indicated that the nanostructure of the TiO_2 particles played a valuable role in their photocatalytic activities. Compared with the commercial P25, our synthesized porous TiO_2 with large amount of pores and extremely high surface areas (235.86 m^2/g) displayed a better behaviour in the photo-degradation of Rh-B.

Supplementary Materials: Figure S1: SEM image of (a) porous TiO_2 and (b) hybrid TiO_2/CDs; Figure S2: (a) EDX spectra of hybrid TiO_2/CDs after CDs incorporation. Inset: SEM image of hybrid TiO_2/CDs. (b-d) EDS mapping profiles of the rectangular area in panel (a) for (b) carbon, (c)titanium and (d) oxygen. Figure S3: UV-Vis spectrums of pure P25 and P25 with CDs. Figure S4: Photoluminescence spectrum of CDs with different excitation (add up-conversion). Figure S5: UV-Vis spectra

of RhB-degradation with (a) P25 and (b) P25/CDs under UV light at different irradiation time. (c) Photocatalytic degradation curves of P25 and P25/CDs at different time under UV light irradiation. (d) Pseudo-first-order fitted degradation of RhB by P25 and P25/CDs.

Author Contributions: H. Gao conceived the idea and guided the whole study. F. Song and H. Gao carried out the experiments, including the preparation of TiO_2 mesoporous particles, carbon dots, TiO_2/CDs photocatalysts. Hao Sun conducted the experiments of SEM, TEM and EDX. Hailong Ma carried out the photocatalytic degradation experiments. All authors were involved in result discussion and manuscript writing. F. Song and H. Gao drafted the manuscript with inputs and comments from all authors

Funding: This research was funded by Fundamental Research Funds of Beihang University (Grant No. KG16007908) and Fundamental Public Welfare Research Funds of Zhejiang Province (KYZ1121004).

Acknowledgments: H. Gao gratefully acknowledges the financial support from Fundamental Research Funds of Beihang University (Grant No. KG16007908) and Fundamental Public Welfare Research Funds of Zhejiang Province (KYZ1121004).

Conflicts of Interest: The authors declare no conflict of interest.

References

1. Martins, N. C. T.; Ângelo, J.; Girão, A. V.; Trindade, T.; Andrade, L.; Mendes, A., N-doped carbon quantum dots/TiO2 composite with improved photocatalytic activity. *Appl. Catal., B* **2016,** *193*, 67-74.
2. Zhuo, S.; Shao, M.; Lee, S.-T., Upconversion and Downconversion Fluorescent Graphene Quantum Dots: Ultrasonic Preparation and Photocatalysis. *ACS Nano* **2012,** *6*, 1059-1064.
3. Xiao, S.; Zhang, D.; Pan, D.; Zhu, W.; Liu, P.; Cai, Y.; Li, G.; Li, H., A chloroplast structured photocatalyst enabled by microwave synthesis. *Nat. Commun.* **2019,** *10*, 1570.
4. Schneider, J.; Matsuoka, M.; Takeuchi, M.; Zhang, J.; Horiuchi, Y.; Anpo, M.; Bahnemann, D. W., Understanding TiO2 photocatalysis: mechanisms and materials. *Chem Rev* **2014,** *114*, 9919-9986.
5. Tamaki, Y.; Furube, A.; Murai, M.; Hara, K.; Katoh, R.; Tachiya, M., Direct Observation of Reactive Trapped Holes in TiO2 Undergoing Photocatalytic Oxidation of Adsorbed Alcohols: Evaluation of the Reaction Rates and Yields. *J. Am. Chem. Soc.* **2006,** *128*, 416-417.
6. Zhao, L.; Chen, X.; Wang, X.; Zhang, Y.; Wei, W.; Sun, Y.; Antonietti, M.; Titirici, M. M., One-step solvothermal synthesis of a carbon@TiO(2) dyade structure effectively promoting visible-light photocatalysis. *Adv Mater* **2010,** *22*, 3317-3321.
7. Rao, N. N.; Dube, S., Photocatalytic degradation of mixed surfactants and some commercial soap/detergent products using suspended TiO2 catalysts. *J. Mol. Catal. A: Chem.* **1996,** *104*, L197-L199.
8. Lu, Y.; Liu, X.-L.; He, L.; Zhang, Y.-X.; Hu, Z.-Y.; Tian, G.; Cheng, X.; Wu, S.-M.; Li, Y.-Z.; Yang, X.-H.; Wang, L.-Y.; Liu, J.-W.; Janiak, C.; Chang, G.-G.; Li, W.-H.; Van Tendeloo, G.; Yang, X.-Y.; Su, B.-L., Spatial Heterojunction in Nanostructured TiO2 and Its Cascade Effect for Efficient Photocatalysis. *Nano Lett.* **2020,** *20*, 3122-3129.
9. Fujishima, A.; Honda, K., Electrochemical Photolysis of Water at a Semiconductor Electrode. *Nature* **1972,** *238*, 37-38.
10. Zhang, P.; Shao, C.; Zhang, Z.; Zhang, M.; Mu, J.; Guo, Z.; Liu, Y., TiO(2)@carbon core/shell nanofibers: controllable preparation and enhanced visible photocatalytic properties. *Nanoscale* **2011,** *3*, 2943-2949.
11. Wang, J.; Shen, Y.; Liu, S.; Zhang, Y., Single 2D MXene precursor-derived TiO2 nanosheets with a uniform decoration of amorphous carbon for enhancing photocatalytic water splitting. *Appl. Catal., B* **2020,** *270*, 118885.
12. Choi, W. Y.; Termin, A.; Hoffmann, M. R., The Role of Metal-Ion Dopants in Quantum-Sized Tio2 - Correlation between Photoreactivity and Charge-Carrier Recombination Dynamics. *J Phys Chem-Us* **1994,** *98*, 13669-13679.
13. Xiang, Q.; Yu, J.; Jaroniec, M., Synergetic Effect of MoS2 and Graphene as Cocatalysts for Enhanced Photocatalytic H2 Production Activity of TiO2 Nanoparticles. *J. Am. Chem. Soc.* **2012,** *134*, 6575-6578.
14. Maarisetty, D.; Mahanta, S.; Sahoo, A. K.; Mohapatra, P.; Baral, S. S., Steering the Charge Kinetics in Dual-Functional Photocatalysis by Surface Dipole Moments and Band Edge Modulation: A Defect Study in TiO2-ZnS-rGO Composites. *ACS Appl. Mater. Interfaces* **2020,** *12*, 11679-11692.
15. Osterloh, F. E., Inorganic Materials as Catalysts for Photochemical Splitting of Water. *Chem. Mater.* **2008,** *20*, 35-54.
16. Lv, X.-J.; Zhou, S.-X.; Zhang, C.; Chang, H.-X.; Chen, Y.; Fu, W.-F., Synergetic effect of Cu and graphene as cocatalyst on TiO2 for enhanced photocatalytic hydrogen evolution from solar water splitting. *J. Mater. Chem.* **2012,** *22*, 18542-18549.
17. Fessi, N.; Nsib, M. F.; Cardenas, L.; Guillard, C.; Dappozze, F.; Houas, A.; Parrino, F.; Palmisano, L.; Ledoux, G.; Amans, D.; Chevalier, Y., Surface and Electronic Features of Fluorinated TiO2 and Their Influence on the Photocatalytic Degradation of 1-Methylnaphthalene. *J. Phys. Chem. C* **2020,** *124*, 11456-11468.
18. Yang, Y.; Zhang, Z.; Fang, W.-H.; Fernandez-Alberti, S.; Long, R., Unraveling the quantum dynamics origin of high photocatalytic activity in nitrogen-doped anatase TiO2: time-domain ab initio analysis. *J. Mater. Chem. A* **2020,** *8*, 25235-25244.
19. Wang, Y.; Saitow, K.-i., Mechanochemical Synthesis of Red-Light-Active Green TiO2 Photocatalysts with Disorder: Defect-Rich, with Polymorphs, and No Metal Loading. *Chem. Mater.* **2020,** *32*, 9190-9200.

20. Wang, J.; Gao, M.; Ho, G. W., Bidentate-complex-derived TiO2/carbon dot photocatalysts: in situ synthesis, versatile heterostructures, and enhanced H2 evolution. *J. Mater. Chem. A* **2014,** *2*, 5703-5709.
21. Kim, Y. K.; Sharker, S. M.; In, I.; Park, S. Y., Surface coated fluorescent carbon nanoparticles/TiO2 as visible-light sensitive photocatalytic complexes for antifouling activity. *Carbon* **2016,** *103*, 412-420.
22. Woan, K.; Pyrgiotakis, G.; Sigmund, W., Photocatalytic Carbon-Nanotube–TiO2 Composites. *Adv. Mater.* **2009,** *21*, 2233-2239.
23. Apostolopoulou, V.; Vakros, J.; Kordulis, C.; Lycourghiotis, A., Preparation and characterization of [60] fullerene nanoparticles supported on titania used as a photocatalyst. *Colloids Surf., A* **2009,** *349*, 189-194.
24. Qi, K.; Selvaraj, R.; Al Fahdi, T.; Al-Kindy, S.; Kim, Y.; Wang, G.-C.; Tai, C.-W.; Sillanpää, M., Enhanced photocatalytic activity of anatase-TiO2 nanoparticles by fullerene modification: A theoretical and experimental study. *Appl. Surf. Sci.* **2016,** *387*, 750-758.
25. Zhang, L.-W.; Fu, H.-B.; Zhu, Y.-F., Efficient TiO2 Photocatalysts from Surface Hybridization of TiO2 Particles with Graphite-like Carbon. *Adv. Func. Mater.* **2008,** *18*, 2180-2189.
26. Yang, H.; Zhai, L.; Li, K.; Liu, X.; Deng, B.; Xu, W., A highly efficient nano-graphite-doped TiO2 photocatalyst with a unique sea-island structure for visible-light degradation. *Catal. Sci. Technol.* **2020,** *10*, 1161-1170.
27. Li, X.; Jiang, Y.; Cheng, W.; Li, Y.; Xu, X.; Lin, K., Mesoporous TiO2/Carbon Beads: One-Pot Preparation and Their Application in Visible-Light-Induced Photodegradation. *Nano-Micro Letters* **2015,** *7*, 243-254.
28. Marinovic, A.; Kiat, L. S.; Dunn, S.; Titirici, M.-M.; Briscoe, J., Carbon-Nanodot Solar Cells from Renewable Precursors. *ChemSusChem* **2017,** *10*, 1004-1013.
29. Gerber, I. C.; Serp, P., A Theory/Experience Description of Support Effects in Carbon-Supported Catalysts. *Chem. Rev.* **2020,** *120*, 1250-1349.
30. Cheng, C.; Lu, D.; Shen, B.; Liu, Y. D.; Lei, J. Y.; Wang, L. Z.; Zhang, J. L.; Matsuoka, M., Mesoporous silica-based carbon dot/TiO2 photocatalyst for efficient organic pollutant degradation. *Micropor Mesopor Mat* **2016,** *226*, 79-87.
31. Gao, H.; Sapelkin, A. V.; Titirici, M. M.; Sukhorukov, G. B., In Situ Synthesis of Fluorescent Carbon Dots/Polyelectrolyte Nanocomposite Microcapsules with Reduced Permeability and Ultrasound Sensitivity. *ACS Nano* **2016,** *10*, 9608-9615.
32. Sun, M.; Ma, X.; Chen, X.; Sun, Y.; Cui, X.; Lin, Y., A nanocomposite of carbon quantum dots and TiO2 nanotube arrays: enhancing photoelectrochemical and photocatalytic properties. *RSC Adv.* **2014,** *4*, 1120-1127.
33. Tian, J.; Leng, Y.; Zhao, Z.; Xia, Y.; Sang, Y.; Hao, P.; Zhan, J.; Li, M.; Liu, H., Carbon quantum dots/hydrogenated TiO2 nanobelt heterostructures and their broad spectrum photocatalytic properties under UV, visible, and near-infrared irradiation. *Nano Energy* **2015,** *11*, 419-427.
34. Li, H.; He, X.; Kang, Z.; Huang, H.; Liu, Y.; Liu, J.; Lian, S.; Tsang, C. H. A.; Yang, X.; Lee, S.-T., Water-Soluble Fluorescent Carbon Quantum Dots and Photocatalyst Design. *Angew. Chem. Int. Ed.* **2010,** *49*, 4430-4434.
35. Wang, Q.; Cai, J.; Biesold-McGee, G. V.; Huang, J.; Ng, Y. H.; Sun, H.; Wang, J.; Lai, Y.; Lin, Z., Silk fibroin-derived nitrogen-doped carbon quantum dots anchored on TiO2 nanotube arrays for heterogeneous photocatalytic degradation and water splitting. *Nano Energy* **2020,** *78*, 105313.
36. Gao, C.; Wei, T.; Zhang, Y.; Song, X.; Huan, Y.; Liu, H.; Zhao, M.; Yu, J.; Chen, X., A Photoresponsive Rutile TiO2 Heterojunction with Enhanced Electron–Hole Separation for High-Performance Hydrogen Evolution. *Adv. Mater.* **2019,** *31*, 1806596.
37. Chen, J.; Shu, J.; Anqi, Z.; Juyuan, H.; Yan, Z.; Chen, J., Synthesis of carbon quantum dots/TiO2 nanocomposite for photo-degradation of Rhodamine B and cefradine. *Diamond Relat. Mater.* **2016,** *70*, 137-144.
38. Kheamrutai Thamaphat*, P. L. a. B. N., Phase Characterization of TiO2 Powder by XRD and TEM. *Kasetsart J. (Nat. Sci.)* **2008,** *42*, 357-361.
39. Hurum, D. C.; Gray, K. A.; Rajh, T.; Thurnauer, M. C., Recombination Pathways in the Degussa P25 Formulation of TiO2: Surface versus Lattice Mechanisms. *The Journal of Physical Chemistry B* **2005,** *109*, 977-980.
40. Kopidakis, N.; Schiff, E. A.; Park, N. G.; van de Lagemaat, J.; Frank, A. J., Ambipolar Diffusion of Photocarriers in Electrolyte-Filled, Nanoporous TiO2. *The Journal of Physical Chemistry B* **2000,** *104*, 3930-3936.
41. Liu, B.; Zeng, H. C., Carbon Nanotubes Supported Mesoporous Mesocrystals of Anatase TiO2. *Chem. Mater.* **2008,** *20*, 2711-2718.
42. Barrett, E. P.; Joyner, L. G.; Halenda, P. P., The Determination of Pore Volume and Area Distributions in Porous Substances. I. Computations from Nitrogen Isotherms. *J. Am. Chem. Soc.* **1951,** *73*, 373-380.
43. Yu, H.; Zhao, Y.; Zhou, C.; Shang, L.; Peng, Y.; Cao, Y.; Wu, L.-Z.; Tung, C.-H.; Zhang, T., Carbon quantum dots/TiO2 composites for efficient photocatalytic hydrogen evolution. *Journal of Materials Chemistry A* **2014,** *2*, 3344.
44. Tasviri, M.; Rafiee-Pour, H.-A.; Ghourchian, H.; Gholami, M. R., Amine functionalized TiO2–carbon nanotube composite: synthesis, characterization and application to glucose biosensing. *Applied Nanoscience* **2011,** *1*, 189-195.